Journal of
Applied Crystallography
ISSN 0021-8898

Received 16 August 2006
Accepted 31 January 2007

Spin-echo small-angle neutron scattering study of the domain structure of an Ni layer on a Cu substrate

Sergey V. Grigoriev,[a]* Yurii O. Chetverikov,[a] Vladimir N. Zabenkin,[a] Wicher H. Kraan,[b] M. Theo Rekveldt[b] and Niels van Dijk[b]

[a]Petersburg Nuclear Physics Institute, 188300 Gatchina, St. Petersburg, Russia, and [b]Dept. R3, Faculty of Applied Sciences, Delft University of Technology, 2629 JB Delft, The Netherlands. Correspondence e-mail: grigor@pnpi.spb.ru

Spin-echo small-angle neutron scattering (SESANS) is used to study the magnetic domain structure of an Ni layer electrodeposited onto a Cu substrate. The domain structure of the sample corresponds to the hard-plane model, where the magnetization in the domains is directed perpendicular to the layer; the domain length coincides with the thickness of the layer of the order of 10 μm and its width is of the order of 1 μm. The pair correlation function of the magnetization has been directly measured. It is established that the width of the domain depends linearly on its thickness. The domain structure does not depend on heating at temperatures below T_C of nickel. Annealing at $T > T_C$ results in a reconstruction of the domain structure with a tendency to the easy-plane model, *i.e.* with domain magnetization in the plane. The multiple scattering effect is studied and may be taken into account. This experiment demonstrates the possibilities of magnetic SESANS. Some aspects of this novel technique are pointed out.

1. Introduction

Spin-echo small-angle neutron scattering (SESANS) is a novel method for determining the structure of materials in real space (Rekveldt, 1996; Bouwman *et al.*, 2004; Rekveldt *et al.*, 2003, 2005). The method is based on the Larmor precession of polarized neutrons transmitted through two successive precession devices before and after the sample, which encodes the scattering angle into a net precession angle. The principal difference of SESANS from conventional SANS is that it measures a real-space function.

Although SESANS has been applied to numerous nonmagnetic systems, it was only recently realized that SESANS can also be used to study magnetic samples (Grigoriev *et al.*, 2006). Magnetic SESANS is based on the same major principles, which were established long ago by Mezei for inelastic scattering in magnetic systems (Mezei, 1980, 2003). We are helped by the fact that the polarization is flipped in the magnetic scattering process, which allows one to eliminate the usual π flipper to observe spin echo. Hence, by taking measurements with and without a flipper from the same sample, magnetic and nuclear modes of scattering can be separated in a trivial way. We point out that without a flipper (*i.e.* in magnetic mode) no signal from *non*magnetic scattering would appear accounting for nonmonochromaticity of real neutron beams. So, the presence of a signal is unambiguous evidence of magnetic neutron scattering. The formalism for magnetic SESANS is similar to that for nonmagnetic SESANS, except for the correction for multiple scattering.

2. Magnetic spin-echo SANS: principles

The principles of the SESANS technique are described in detail in a number of papers (Rekveldt, 1996; Rekveldt *et al.*, 2005). The central feature to be taken into account in magnetic SESANS is the change of the polarization at the very process of scattering. For ferromagnetic samples the polarization $\mathbf{P}_s$ of the scattered neutrons is given by Izyumov & Ozerov (1970):

$$\mathbf{P}_s = 2\mathbf{m}_\perp(\mathbf{m}_\perp \cdot \mathbf{P}_0) - \mathbf{P}_0, \tag{1}$$

where $\mathbf{m}_\perp = \mathbf{m} - (\mathbf{m} \cdot \hat{\mathbf{q}})\hat{\mathbf{q}}$. $\hat{\mathbf{q}}$ is the unit scattering vector, $\mathbf{m}$ is the unit magnetization vector and $\mathbf{P}_0$ is the polarization just before the scattering. The last equation shows that for neutrons scattered at $\mathbf{q} \perp \mathbf{m}$ the polarization component parallel to the local magnetization, $P_{0\|}$, remains unchanged in the scattering process, while the component perpendicular to it, $P_{0\perp}$, changes its sign. In this case there is in principle no polarization loss (at least in the single scattering approximation) as happens in paramagnetic scattering, where $\mathbf{P}_s = -\hat{\mathbf{q}}(\hat{\mathbf{q}} \cdot \mathbf{P}_0)$. Let us consider the situation when the local magnetization is directed along the propagation axis x and the polarization is in the plane (xz). As a consequence, to observe the NSE signal a flipper between the spin echo arms is not needed. So, by switching on or off the flipper one can separate the magnetic scattering from other contributions, in particular, from the nuclear one and from the unscattered beam.

As shown in Grigoriev *et al.* (2006), the polarization measured in magnetic SESANS in the single scattering approximation is

$$P_m = P_0 x\sigma G(Z), \tag{2}$$

where $x\sigma = x/l_f$ is a dimensionless sample thickness normalized on the mean free path of the neutron l_f, $\sigma = 1/l_f$ is the total magnetic neutron cross section and the function $G(Z)$ is given by

$$G(Z) = \int \mathrm{d}x \langle \rho_\mathrm{m}(r)\rho_\mathrm{m}(r+Z)\rangle = \frac{1}{\sigma k_0^2}\int \mathrm{d}Q_y\ \mathrm{d}Q_z \frac{\mathrm{d}\sigma}{\mathrm{d}\Omega(Q)}\cos(Q_z Z). \tag{3}$$

$\rho_\mathrm{m}(r)$ is the magnetic scattering potential. The instrumental quantity Z defines a length called the 'spin-echo length' and it is given by

$$Z = (c\lambda^2 BL\cot\theta_0)/2\pi. \tag{4}$$

This length can be scanned by varying the neutron wavelength λ, the magnetic field B, the length of the spin-echo device L or the inclination angle θ_0.

In case of multiple scattering one should realise that the second scattering event either reverses the polarization again or leads to partial depolarization. In this case, the number of neutrons scattered once is decreased by those scattered twice. Then one can rewrite equation (2) in the following form:

$$P_\mathrm{m} = P_0 G(Z)(x\sigma)\exp(-x\sigma). \tag{5}$$

Thus the measured polarization P_m is proportional to the function $G(Z)$ and multiple scattering appears now as the factor $\exp(-x\sigma)$. Equation (5) shows that the amplitude of the NSE signal is a function of the normalized thickness $x\sigma$ of the sample: $F(x\sigma) = (x\sigma)\exp(-x\sigma)$. Its maximum occurs at $x\sigma = 1$ and is equal to $1/e$.

For magnetic scattering it is rather simple to normalize the amount of scattering. According to Maleyev & Ruban (1972) and Maleyev (1982), the depolarization of the transmitted beam, which is not in spin-echo mode, is a measure for the total magnetic cross section:

$$P_\mathrm{m}/P_0 = \exp(-l\sigma) = \exp\left[-l\frac{1}{k_0^2}\int \mathrm{d}Q_y\ \mathrm{d}Q_z\left(\frac{\mathrm{d}\sigma}{\mathrm{d}\Omega(Q)}\right)\right], \tag{6}$$

where the initial polarization $\mathbf{P}_0$ is parallel to the incident beam. We note here that the expressions above are valid in the Born approximation of scattering by magnetic domains or inhomogeneities. The criterion of its applicability (the diffraction limit) can be formulated as the condition that the angle of precession of the polarization vector in the magnetic field $\mathbf{B}_\mathrm{d}$ of a domain with size R_d along the beam axis has to be small:

$$c\lambda B_\mathrm{d} R_\mathrm{d} \ll 2\pi. \tag{7}$$

At the same time, as shown in Halperin & Holstein (1941), in approximation (7) the polarization of a neutron beam transmitted through the sample decreases with wavelength as $\exp(\alpha\lambda^2)$. When the opposite inequality holds, the depolarization of the neutrons is independent of wavelength. Therefore, the experimentally measured λ^2 dependence of the polarization should indicate whether or not condition (7) is satisfied and the diffraction limit is applicable.

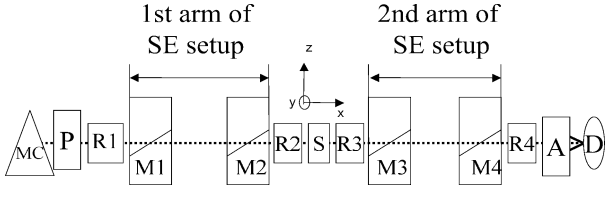

Figure 1
Schematic drawing of the SESANS setup at IRI TU Delft: MC monochromator crystal; P polarizer; R1, R2, R3 and R4 polarization rotators; M1, M2, M3 and M4 electromagnets; S sample position; A analyser; D detector. The system consisting of M1 and M2 makes up the first arm of a spin-echo setup; M3 and M4 make up its second arm.

3. Experimental

Samples of ferromagnetic Ni layers of different thickness electrodeposited on a copper substrate were used for this study. It is known [see Kraan & Rekveldt (1977) and references therein] that the domain structure of these samples corresponds to the hard-plane model when the magnetization in the domains is directed perpendicular to the layer; the domain length coincides with the thickness of the layer of the order of 10 μm and its width is of the order of 1 μm.

We exploited the SESANS instrument at IRI in Delft (Rekveldt *et al.*, 2005), schematically shown in Fig. 1. A polarized neutron beam with λ = 0.21 nm and $\Delta\lambda/\lambda$ = 0.01 was used. The basic components are electromagnets M1–M4 with 9 μm-thick permalloy films positioned at $\theta_0 = 5.5^\circ$ to the neutron beam at the centre of the rectangular poles of these electromagnets. Their fields are set and controlled by software to values usually between 1 and 130 mT. These settings allow one to scan the spin-echo length Z from 0.1 to 10 μm. The sample S is mounted between the two SE arms. Two $\pi/2$ rotators of polarization R2 and R3 are installed around the sample position in order to set the polarization into the (xz) plane.

A typical example of a SESANS curve is given in Fig. 2. Fig. 2(a) shows the polarization measured as a function of the parameter Z for the 'nuclear' mode. In this mode the nuclear SESANS correlation function is measured. We see no variation of P, demonstrating the absence of nuclear inhomogeneities in the sample. Due to magnetic scattering, the level of the polarization is equally suppressed for all Z. According to equation (5) this depolarization gives the total magnetic scattering.

Fig. 2(b) shows the polarization for the 'magnetic' mode. For this mode, the sign of the field was not actually reversed, but we arranged an adiabatic transition between M2 and M3 that compensates for the action of the field reversal. The polarization shows a damped oscillating behaviour as a function of Z with a minimum at Z = 3 μm and a maximum at Z = 6 μm. According to equation (5), $P(z)$ is proportional to the pair correlation function $G(z)$ [equation (3)]. The maximum and minimum in Fig. 2(b) show that neighbouring domains of the collinear and opposite magnetization directions are correlated at a distance of 6 and 3 μm, respectively. One can conclude, therefore,

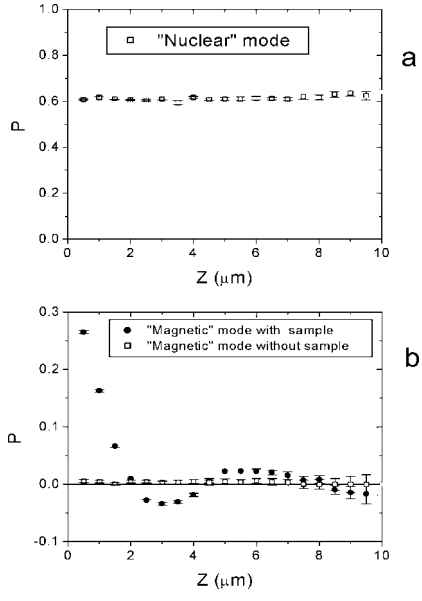

Figure 2
Polarization measured as a function of the spin-echo length Z for the 'nuclear' (a) and 'magnetic' (b) modes (see text for details).

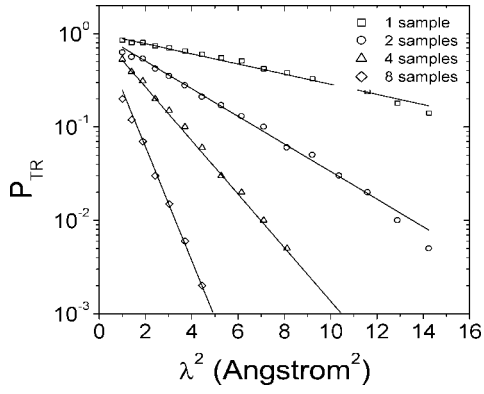

Figure 3
Polarization on a log scale as a function of the neutron wavelength squared λ^2 measured in nuclear mode for the different numbers of samples $N = 1, 2, 4, 8$.

that the characteristic size of the domain is $D = 3$ μm. The linear character of the dependence $P(Z)$ at small $Z < 2$ μm is typical for the autocorrelation function of the cylinder-like particles oriented parallel to the neutron beam and perpendicular to the plane of the Ni layer. This fact supports the assumption about the hard-plane model. For comparison we also plot the polarization in the 'magnetic' mode without a sample. As expected, it is close to zero because the precessions in both arms add, since the spin flip during a magnetic scattering event is absent.

4. Results

4.1. Applicability of the scattering approach

To prove the applicability of the scattering approach in magnetic SESANS we performed measurements of the neutron depolarization of the transmitted beam as a function of the wavelength λ. In Fig. 3 the polarization on a log scale is plotted against λ^2 for a different number of foils positioned in place of the sample. All curves demonstrate a linear dependence proving that inequality (6) holds and our experiments stay well within the diffraction limit. On the other hand, one can estimate from Fig. 3 and equation (6) that the neutrons become doubly scattered for $N = 8$ foils and wavelength λ = 2 Å. Thus the problem of multiple scattering is of importance.

Fig. 4 shows the pair correlation function measured for the different numbers of samples $N = 1, 2, 3$. One can see that the shape

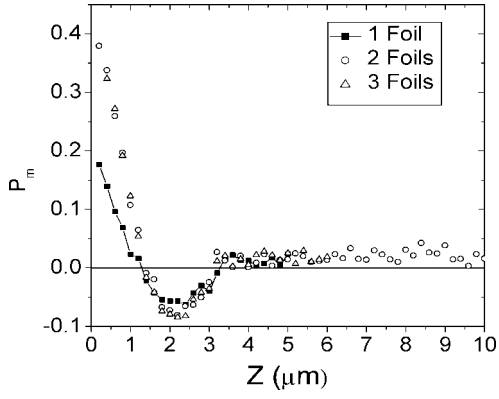

Figure 4
Polarization measured as a function of the spin-echo length Z in the 'magnetic' mode for the different numbers of samples $N = 1, 2, 3$.

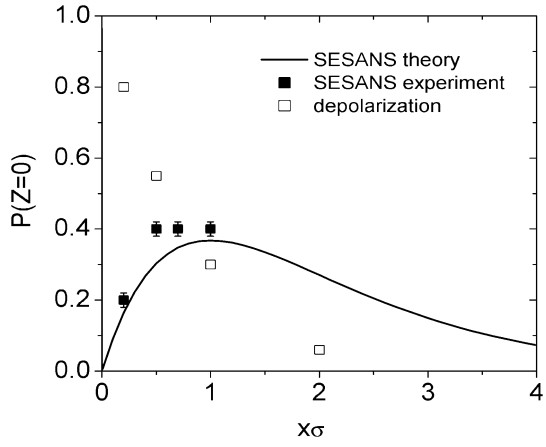

Figure 5
Amplitude of the spin-echo signal A_{SESANS} and polarization of the transmitted beam P_{TR} as a function of the thickness x of the sample normalized by the mean free path $l_f = 1/\sigma$. Points are obtained from experiment; lines are from the theoretical prediction.

of the curve (both the linear dependence at small Z and the position of the minimum) does not depend on the number of foils but it can be scaled with a certain factor in good agreement with equation (5). The amplitude of the signal $P(Z \rightarrow 0)$ is plotted in Fig. 5. It follows roughly the theoretical prediction shown as a line in Fig. 5. The depolarization for λ = 2 Å is plotted in Fig. 5 for comparison. Figs. 4 and 5 demonstrate the applicability of the theoretical approach presented above.

4.2. Thickness dependence

SESANS curves were measured for samples with different thicknesses. Fig. 6 shows the polarization as a function of the spin-echo length Z for sample thicknesses of 10, 15 and 21 μm. It is seen that all curves have a similar shape but are differently scaled on both the P and Z axes. The correlation length for the domain structure or width of the domains, determined as Z_{min}, changes from sample to sample. Fig. 7 shows the relation between the thickness of the layer L and the width of the domain D. The data show a linear dependence with the thickness-to-width ratio equal to $L/D = 5.1$.

4.3. Temperature evolution

The pair correlation function was measured for the sample with thickness 21 μm for different temperatures from $T = 300$ K up to $T_C = 630$ K. Fig. 8 shows the SESANS curves taken at $T = 373$, 523 and

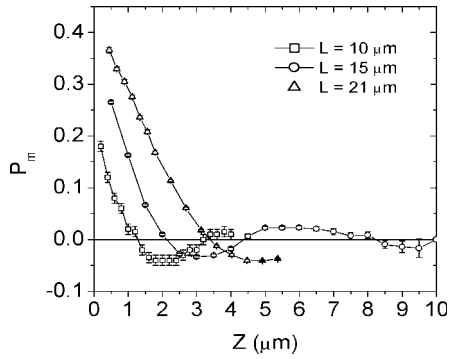

Figure 6
Polarization measured as a function of the spin-echo length Z for the sample thicknesses 10, 15 and 21 μm.

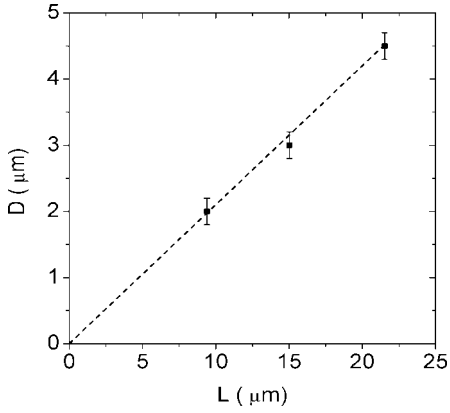

Figure 7
The width of the domain D plotted as a function of the thickness of the layer L.

573 K. It is seen that the curves at different temperatures are scaled differently on the P axis but their shape does not change. Therefore one can conclude that the width of the domains is temperature independent and this domain structure is frozen during manufacturing the sample by electrodeposition of Ni on the Cu substrate. The amplitude of the signal, determined as $P(Z \rightarrow 0)$, decreases with increase of temperature (filled symbols in Fig. 9). We have also plotted in Fig. 9 the value of the depolarization of the transmitted beam taken in nuclear mode measurements (empty symbols). The amplitude of the SESANS signal is close to the value of the depolarization of the transmitted beam. Thus we demonstrate that the depolarization caused by the ferromagnetic structure is not the factor to be avoided in magnetic SESANS but it is the phenomenon under study. The magnitude of the SESANS signal is of the same order as or equal to the value of the depolarization.

Fig. 10 shows the pair correlation function of the domain structure after annealing at 650 K and cooling down to 300 K. As seen from Fig. 10, the shape of the curve is strongly deformed after annealing. The curve consists of two parts. The first part is attributed to the scattering by the domains magnetized perpendicular to the sample plane – as it was before the annealing – with a size of the order of 2 μm. The second part is attributed to the domains magnetized in the plane with a size of the order of 10 μm. Thus one may conclude that annealing at $T > T_C$ results in a reconstruction of the domain structure with a tendency to the easy-plane model.

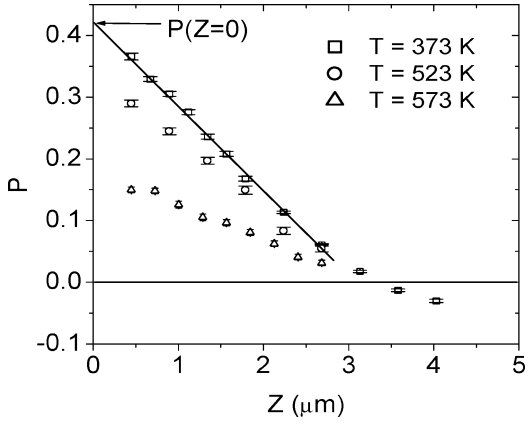

Figure 8
Polarization measured as a function of the spin-echo length Z for the sample of thickness 21 μm at T = 373, 523 and 573 K.

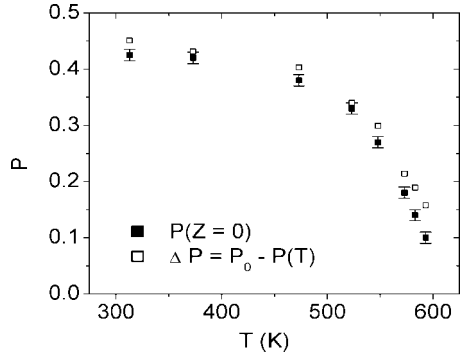

Figure 9
The temperature dependence of the amplitude of the SE signal and the level of depolarization for the 21 μm thick sample.

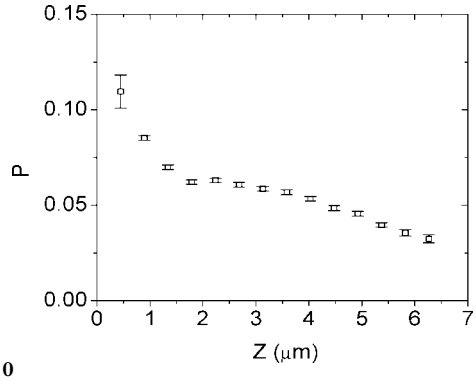

Figure 10
Polarization measured as a function of the spin-echo length Z for the sample with thickness 15 μm after annealing at 650 K and cooling down to 300 K.

5. Summary and outlook

Magnetic SESANS is a promising technique for the investigation of: (i) ferromagnetic materials for industry (magnetic memory devices, magnetic steel *etc.*); (ii) magnetic temperature phase transitions (magnetic memory alloys, gigantic magneto-resistance materials, ferromagnetic Invars *etc*); and (iii) magnetic quantum phase transitions under applied pressure.

In order to realise the applications described above, this technique needs to be developed as follows. Firstly, the sample environment has to be designed to work with the magnetic field. Secondly, it has to allow the temperature of the sample to be varied from low values using a cryostat up to high values using an oven to study temperature phase transitions. Thirdly, for studying quantum phase transitions the sample environment has to be designed to allow the use of a pressure cell at room temperature and at low temperatures.

In summary: magnetic SESANS promises to have a large number of both industrial and fundamental applications.

One of the authors (SG) thanks NWO for a grant that enabled him to perform this work in the Faculty of Applied Science of TU Delft. The work was partly supported by INTAS foundation (grant No. INTAS-03-51-6426) and RFFR (project 05-02-16558). The research project has been partially supported by the European Commission under the 6th Framework Programme through the Key Action: Strengthening the European Research Area, Research Infrastructures, contract No RII3-CT-2003-505925.

References

Bouwman, W. G., Krouglov, T. V., Plomp, J., Grigoriev, S. V., Kraan, W. H. & Rekveldt, M. Th. (2004). *Physica B*, **350**, 140–146.

Grigoriev, S. V., Kraan, W. H., Rekveldt, M. Th., Kruglov, T. & Bouwman, W. G. (2006). *J. Appl. Cryst.* **39**, 252–258.
Halperin, O. & Holstein, T. (1941). *Phys. Rev.* **59**, 960–978.
Izyumov, Y. A. & Ozerov, R. P. (1970). *Magnetic Neutron Diffraction*, pp. 171–176. New York: Plenum Press.
Kraan, W. H. & Rekveldt, M. Th. (1977). *J. Magn. Magn. Mater*, **5**, 247–257.
Maleyev, S. V. (1982). *J. Phys. C*, **7**, 23–26.
Maleyev, S. V. & Ruban, V. A. (1972). *Zh. Eksp. Teor. Fiz.* **62**, 416–422.
Mezei, F. (1980). *Neutron Spin Echo. Lecture Notes in Physics*, Vol. 128, pp. 3–26. Berlin: Springer-Verlag.
Mezei, F. (2003). *Neutron Spin Echo. Lecture Notes in Physics*, Vol. 601, edited by F. Mezei, C. Pappas & T. Gutberlet, pp. 5–14. Berlin: Springer-Verlag.
Rekveldt, M. Th. (1996). *J. Nucl. Instrum. Methods B*, **114**, 366–370.
Rekveldt, M. Th., Bouwman, W. G., Kraan, W. H., Uca, O., Grigoriev, S. V., Habich, K. & Keller, T. (2003). *Neutron Spin Echo. Lecture Notes in Physics*, Vol. 601, edited by F. Mezei, C. Pappas & T. Gutberlet, pp. 87–99. Berlin: Springer-Verlag.
Rekveldt, M. Th., Plomp, J., Bouwman, W. G., Kraan, W. H., Grigoriev, S. & Blaauw, M. (2005). *Rev. Sci. Instrum.* **76**, 033901-9.